Fluorescence of bimolecular guanine quadruplexes: from femtoseconds to nanoseconds

Evangelos Balanikas, Thomas Gustavsson, Dimitra Markovitsi

Fluorescence of Bimolecular Guanine Quadruplexes: From Femtoseconds to Nanoseconds

Evangelos Balanikas,[1] *Thomas Gustavsson*[1] *and Dimitra Markovitsi*[1,2*]

1 Université Paris-Saclay, CEA, CNRS, LIDYL, F-91191 Gif-sur-Yvette, France

2 Université Paris-Saclay, CNRS, Institut de Chimie Physique, UMR8000, 91405 Orsay, France

email. dimitra.markovitsi@universite-paris-saclay.fr

KEYWORDS. Guanine Quadruplexes, DNA, Oxytricha, Intrinsic Fluorescence, Femtosecond spectroscopy

ABSTRACT. The paper deals with the fluorescence of guanine quadruplexes (G4) formed by association of two DNA strands d(GGGGTTTTGGGG) in the presence of K^+ cations, noted as OXY/K^+ in reference to the protozoon *oxytricha nova*, whose telomere contains TTTTGGGG repeats. They were studied by steady-state and time-resolved techniques, time-correlated single photon counting and fluorescence upconversion. The maximum of the OXY/K^+ fluorescence spectrum is located at 334 nm and the quantum yield is 5.8×10^{-4}. About 75% of the photons are emitted before 100 ps and stem from $\pi\pi^*$ states, possibly with a small contribution of charge transfer. Time-resolved fluorescence anisotropy measurements indicate that ultrafast (< 330 fs) excitation transfer, due to internal conversion among exciton states, is more efficient in OXY/K^+ compared to previously studied G4 structures. This is attributed to the arrangement of the peripheral thymines in two diagonal loops with restricted mobility, facilitating the interaction among them and with guanines. Thymines should also be responsible for a weak intensity excimer/exciplex emission band, peaking at 445 nm. Finally, the longest living fluorescence component (~2.1 ns) is observed at the blue side of the spectrum. So far, high-energy long-lived emitting states had been reported only for double-stranded structures but not for G4.

Introduction

Guanine quadruplexes (G4) are non-canonical DNA/RNA structures playing a central role in several biological functions, such as replication, transcription, carcinogenesis, aging, and apoptosis.[1] They are also used as targets in cancer therapy.[2] Moreover, due to their stability and their programmable self-assembling properties, they are extensively studied for applications in

the field of nanotechnology.[3] Recently, their intrinsic fluorescence has started to be investigated for the development of biosensors.[4,5] In this respect, a better understanding of the factors that affect the G4 fluorescence is necessary.

The intrinsic fluorescence of nucleic acids in general (mononucleotides, single and double strands) is very weak, with the associated quantum yields ϕ being of the order of 10^{-4},[6] because of highly efficient non-radiative deactivation channels.[7] Yet, ϕ values higher by an order of magnitude have been determined for certain G4.[6,8]

The building blocks of G4 are the G-tetrads, composed of four guanines interconnected via Hoogsteen hydrogen bonds (Figure 1a). Vertically stacked G-tetrads constitute the G-core. In addition, peripheral nucleobases may be located at loops linking the G-tetrads among them, or appear as ending groups.[9] The latter were found to affect the fluorescence properties of G4, along with their topology or the type of the metal cations in their central cavity.[6,10-15] Another important structural characteristic of G4 is their molecularity.[9] They may be formed by folding of a single, guanine rich, DNA/RNA strand (monomolecular G4) or the association of two, three or four strands, giving rise to bimolecular, trimolecular or tetramolecular structures, respectively. The fluorescence studies performed up to now concern only monomolecular and tetramolecular G4.

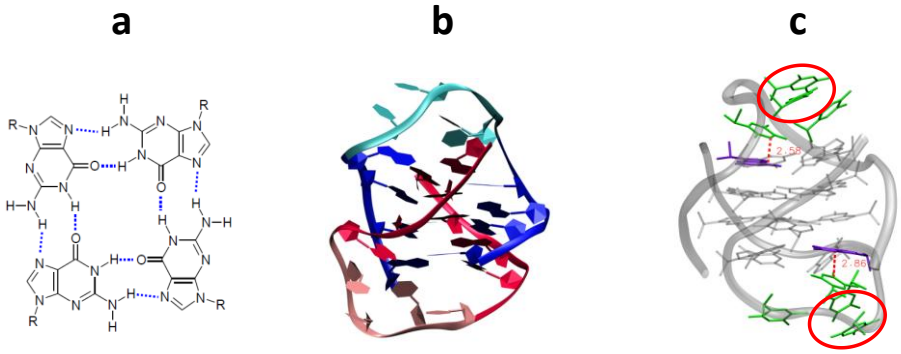

Figure 1. Schematic illustration of the G-tetrad (a) and the studied bimolecular OXY/K^+ structure (b and c; pdb 1K4X from reference 16). In (b) one strand is represented in blue-green colors while the other in red-brown colors with thymines in turquoise and pink, respectively. In (c) thymines are shown in green and two guanines nearly stacked with a thymine of each loop in violet; two pairs of nearly stacked thymines per loop are encircled in red.

Here, we report the first fluorescence study of bimolecular G4. We focus on G4 formed by association of two d(GGGGTTTTGGGG) strands in the presence of potassium cations,[16] abbreviated as OXY/K^+ (Figure 1b). The "OXY" notation is derived from *oxytricha nova*, a protozoon whose telomere contains repeats of the TTTTGGGG sequence. The structure of OXY/K^+ has been extensively studied by X-ray diffraction,[17] NMR spectroscopy,[16,18] CD spectroscopy and Raman spectroscopy[19] as well as molecular dynamics simulations.[20,21]

Our approach, based on time-resolved fluorescence spectroscopy, goes beyond the phenomenological approach of the steady-state fluorescence spectroscopy. It provides information not only about the temporal features of the electronic transitions involved in photon emission, but also about their polarization. The time-resolved study was performed using femtosecond laser pulses at 267 nm as excitation source (indicated by a vertical line in Figure 2a). Detection from the femtosecond to the nanosecond timescales was achieved by combining two different techniques, fluorescence upconversion (FU) and time-correlated single photon counting (TCSPC). We recorded fluorescence decays and fluorescence anisotropies r(t) at selected wavelengths (indicated by vertical lines in Figure 2b).

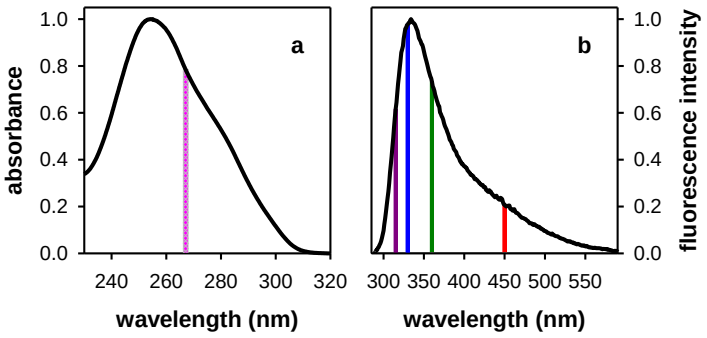

Figure 2. Steady-state absorption (a) and fluorescence (b) spectra of OXY/K^+. Vertical bars indicate the excitation (a: 267 nm) and emission (b: 315, 330, 360 and 450 nm) wavelengths probed in the time-resolved experiments.

Femtosecond experiments are essential for the study of DNA systems because almost always the largest percentage of photons are emitted at time-scales that cannot be resolved by TCSPC; and inversely, weak amplitude long-lived components that could play an important role in photoreactivity, go undetectable by FU.[6] So far, only two types of G4, monomolecular ones formed by the sequence d(GGGATTGGGATTGGGATTGGG) (TEL21) and tetramolecular ones composed of four d(TG_nT) strands, have been studied by time-resolved fluorescence spectroscopy over such a large time-domain.[13,22-26]

The fluorescence properties of OXY/K^+ determined in this work are discussed in the light of those reported for $(TG_4T)_4/K^+$ ten years ago;[23] The two G4 structures are composed of exactly the same nucleobases, but arranged in a different way.

Results

OXY/K^+ was studied in phosphate buffer (pH 7). The G4 preparation, the experimental setups and the operating conditions are described in detail in the Supporting Information (SI). Here we simply stress two points that are crucial for the study of DNA systems whose ϕ is extremely low. First, the oligonucleotides were purified by reversed phase HPLC and controlled by MALDI-TOF. In addition, the purity of the salts used for the preparation of the solutions was higher than 99.99%. Second, particular caution was taken during the experiments so that to avoid detecting fluorescence from photodamaged G4.

The fluorescence maximum of OXY/K^+ is located at 334 ± 2 nm, the same as that reported for the stoichiometric mixture of the constitutive mononucleotides 2'-deoxyribose guanine

monophosphate (dGMP) and TMP (33 ± 2).[23] Yet, ϕ is clearly higher: 5.8×10^{-4} versus 1.3×10^{-4} for the monomer mixture.

The fluorescence decays recorded by FU over two different time-scales (Figure 3) slow down upon increasing the emission wavelength, but the variations are not very large. Since no rise could be observed in the red region, this trend cannot be explained as a spectral shift. Focusing on the signal at 330 nm, close to the fluorescence maximum, we observe that at 8 ps it has lost about 80% of its amplitude, while at 70 ps only *ca.* 0.02% persists.

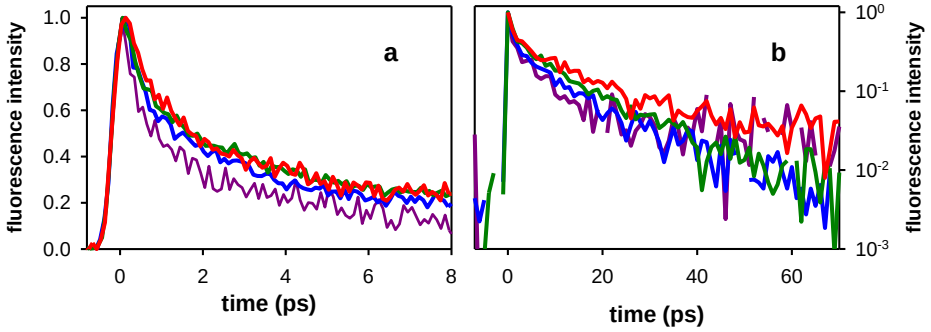

Figure 3. Normalized fluorescence decays recorded for OXY/K^+ by FU at 315 nm (violet), 330 nm (blue), 360 nm (green) and 450 nm (red) on two different time-scales (a and b).

The fluorescence decays recorded by TCSPC (Figure 4) exhibit a more complex wavelength dependence compared to the FU curves. The decay at 330 nm attains the zero level within about 1 ns, and hardly any photons are emitted on the ns time-scale (Figure 4a). In contrast, at the three other wavelengths, longer components are present. However, the dynamics at shorter and longer wavelengths are quite distinct. The decay at 315 nm starts out as fast as at 330 nm but slows gradually down, presenting a long tail extending to several ns. Slower decays are also observed at 360 and 450 nm (Figure 4b), but, at times longer than ~2 ns, their relative amplitude becomes lower than that of the 315 nm signal (Figure 4c).

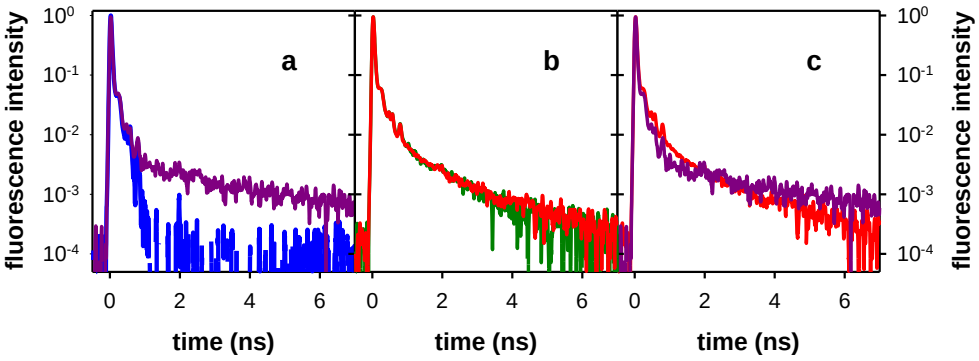

Figure 4. Comparison of the normalized fluorescence decays recorded for OXY/K^+ by TCSPC at 315 nm (violet, a and c), 330 nm (blue, a), 360 nm (green, b) and 450 nm (red, band c). The zero-time was arbitrarily set at the maximum of the signals.

We fitted separately the signals obtained by FU and TCSPC using exponential model functions (see SI for details). As explained in reference 6, the time constants derived from such fits cannot be directly associated with specific excited states because of the anisotropic nature of the studied system and the conformational motions occurring on the probed time-scales. Yet, they allow making some quantitative comparisons. Average lifetimes determined by FU, $\langle\tau^{FU}\rangle$, as well as the longest time constants derived from the TCSPC signals, $\langle\tau_{long}^{TCSPC}\rangle$, are presented in Tables S1 and S2, respectively. These corroborate the phenomenological observations made above: $\langle\tau^{FU}\rangle$ increase with the emission wavelength, with the exception that the value at 315 nm is slightly longer than those around the fluorescence maximum. In contrast, the largest $\langle\tau_{long}^{TCSPC}\rangle$ value is encountered at 315 nm (2.1 ns).

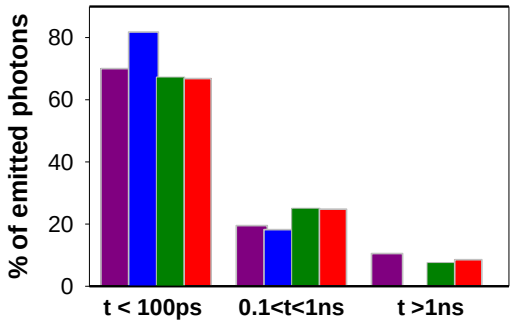

Figure 5. Percentage of photons emitted by OXY/K^+ at 315 nm (violet), 330 nm (blue), 360 nm (green) and 450 nm (red) on three successive time-domains.

Using the TCSPC data, we determined the percentage (%) of photons emitted at each wavelength per decade of time, illustrated in the form of histograms in Figure 5. For all the probed wavelengths, at least 65% of the photons are emitted before 100 ps; 25% of the photons emitted at 360 and 450 nm are encountered on the 0.1 ns to 1 ns range, while somewhat lower values are found for the shorter wavelengths. Finally, between 1 and 9.5 ns (signals become too noisy after the latter time), the largest percentage of photons (10.5 %) is found for 315 nm, which is higher than the values determined for 360 nm (7.6 %) and 450 nm (8.5 %). The percentage of photons emitted at 330 nm after 1 ns falls within the error bar, estimated to ±0.5%. Taking into account the percentage of photons emitted at each probed wavelength and the relative intensity of the florescence spectrum at the considered wavelength, we estimate that 75% of the OXY/K^+ fluorescence is emitted before 0.1 ns.

The histograms in Figure 5 can also be viewed as very rough time-resolved spectra. They indicate that below 0.1 ps the maximum coincides with that of the steady state emission spectrum. Subsequently, emission at longer wavelengths becomes preponderant. Finally, we have an inversion on the ns time-scale, with the emission at 315 nm being more important.

Turning to the time-resolved fluorescence anisotropy (Figure 6), the following observations can be made. First, we remark that on the sub-ps time-scale (Figure 6a) the r(t) values found for OXY/K^+ are significantly lower than those corresponding to a stoichiometric mixture of dGMP and TMP, with zero-time values (r_0) being 0.14 and 0.27, respectively. This comparison precludes the possibility that the low r_0 value found for OXY/K^+ is due to physical motions of the chromophores, since we deal with a much larger and more rigid system than the mononucleotides. Hence, it points toward an electronic origin, which will be discussed in the next section. On the subsequent time-scale (Figure 6b), the 330 and 360 nm signals do not seem to evolve substantially, fluctuating between 0.04 and 0.08, while that at 450 nm goes on decreasing till 4 ps. Due to the important noise, fluctuations are larger on the 7 - 25 ps range where, however, it is clear that r(t) remains positive (Figure 6c). This is also in line with the r(t) determined by TCSPC at 0.1 ns at 360 and 450 nm (Figure 6d); at longer times, r(t) progressively approaches zero. Even in this case, such a depolarization cannot originate only from rotational diffusion, considering that the characteristic time for the rotational diffusion of $(TG_4T)_4/K^+$, whose size is similar to that of OXY/K^+, was estimated to be of 4.7 ns.[23]

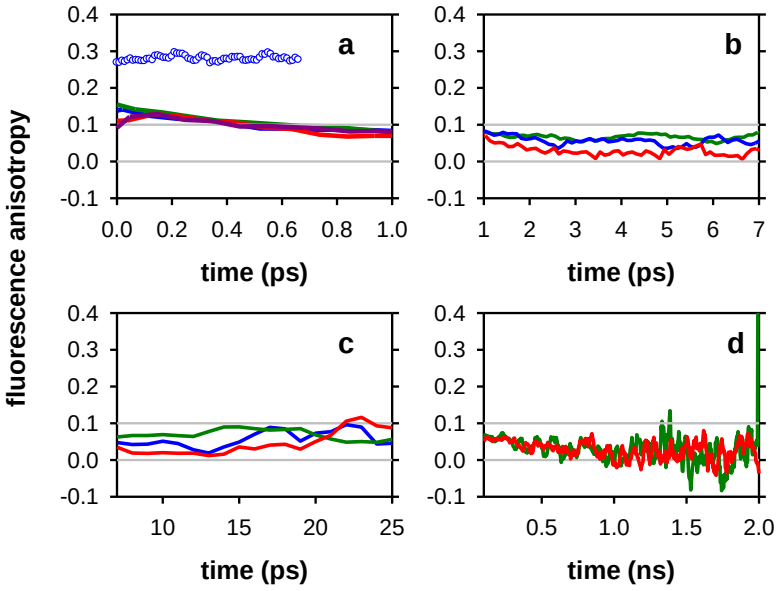

Figure 6. Fluorescence anisotropy traces recorded by FU (a, b and c) and TCSPC (d) at 315 nm (violet), 330 nm (blue), 360 nm (green) and 450 nm (red) on different time-scales. Solid lines: for OXY/K^+, circles: stoichiometric mixture of mononucleotides (dGMP/TMP = 2/1). Signals that are too noisy on the longer time-scales have been omitted. Grey lines correspond to the limiting values of 0.1 and 0.0.

Discussion

General considerations. Before discussing the OXY/K^+ fluorescence, we briefly recall what is known about the excited states of G4 in general. Theoretical calculations on smaller structures reported that the Franck Condon states are delocalized over at least two guanines.[26-32] Two quantum chemistry studies described excited state relaxation in a G4 frame, showing that localization of Frenkel excitons as well charge transfer (CT) between stacked nucleobases may take place.[26,29]

Coming to experimental studies, we stress that fully developed CT excited states, in which an entire atomic charge is transferred from one chromophore to the other, do not contribute to fluorescence because the associated oscillator strength is zero. However, TCSPC is capable of probing weak emission from excited states with a relatively important (though not total) CT character; it is identified by its negative anisotropy, due to the presence of an out-of-plane

component in their emission transition dipole.[6] We stress that FU detects only emission associated with bright excited states, ππ*, possibly containing some weak CT character.[26,33]

Bright excited states and energy transfer. Focusing on OXY/K^+, we saw in the previous section that ~75% of the photons are emitted before 100 ps, suggesting that they stem mainly from excited states with dominant ππ* character. This is in line with the position of the intensity maximum, which coincides with that of the stoichiometric mixture of non-interacting mono-nucleotides and further supported by the fluorescence anisotropy detected by FU (see below). However, the average lifetime $<\tau_{FU}>$ found for OXY/K^+ at 330 nm (4.4 ps, Table S1) is one order of magnitude longer than the corresponding values of non-interacting monomers, 0.64 ps of dGMP and 0.50 ps for TMP.[34] We note that for all the G4 structures studied previously, the lifetimes of the ππ* emission was found to be longer compared to their monomeric constituents.[13,22-26] The ultrafast decays of the monomer fluorescence is explained by the existence of conical intersections joining the potential energy surfaces of the first excited state with the ground state.[7] Quantum chemistry calculations showed that, in the case of dGMP, the process is accompanied by an out-of-plane movement of the amino group.[35] Within the tetrads, the amino groups are engaged in Hoogsteen bonding (Figure 1a), which may slow down the process. An additional reason for the longer living ππ* fluorescence could be the persistent delocalization of the excitation, due to the rigidity of the system.

The initial fluorescence anisotropy, r_0, determined for both OXY/K^+ and the non-interacting mononucleotides is lower than the 0.4, corresponding to the limiting value encountered when photon absorption and emission are parallel. In the case of the monomeric chromophores, the low r_0 value observed is due to a $S_2 \rightarrow S_1$ internal conversion occurring for dGMP when excited at 267 nm.[34] In G4, on the other hand, the internal conversion corresponds to an evolution within

the band formed by the numerous exciton states of the system. Transient absorption experiments showed that intraband scattering in polyadenine strands d(A_{20}) occurs in less than 100 fs,[36] which is below the time-resolution of our FU setup. Given that each exciton state is characterized by its own topography (*i.e*. the nucleobases over which it is delocalized; see figure 9 in reference [27]) and transition moment direction, intraband scattering, occurring before the onset of chromophore motions, gives rise to ultrafast energy transfer among nucleobases. This is reflected in the low initial fluorescence anisotropy, r_0 (Figure 6a). Similar ultrafast decays of r(t) have been reported for all the other G4 studied in this respect. However, the r_0 value determined for OXY/K^+ is the lowest one detected so far for any G4.[13,17-21]

We note that emission associated with a large number of transition dipoles randomly distributed within a plane (like the G-tetrad) results in a r(t) value equal to 0.1.[37] This limiting value is attained for OXY/K^+ within 0.5 ps (Figure 6a). The subsequent decrease of r(t) could arise from the emission of excited states with weak CT character and/or small deviations of the nucleobases from the average G-tetrad plane.[16] Finally, we remark that r(t) remains positive, even on the sub-ns time scale, unlike what was found for other G4 structures, $(TG_4T)_4/Na^+$,[23] TEL21/K^+,[25] TEL21/Na^+.[26] It is worth-noticing that no negative r(t) was detected for $(TG_4T)_4/K^+$ either.[23] This means that excited states with relatively strong CT character do not contribute to the fluorescence of these systems. The reason could be that either such states are not at all populated, or, on the opposite, they evolve very rapidly towards "ideal" CT states, which do not emit at all. This question could be disentangled through transient absorption measurements.

Comparison between OXY/K^+ and $(TG_4T)_4/K^+$. As mentioned in the introduction, OXY/K^+ and $(TG_4T)_4/K^+$ are composed of the same nucleobases, 12 guanines and 8 thymines, but arranged in a different way. The two structures do not exhibit the same topology: the four strands

in $(TG_4T)_4/K^+$ are all parallel,[38] while the two strands in OXY/K^+ are folded in an antiparallel way.[16] These distinct topologies, imposed by the backbone in the presence of K^+ cations, determine the guanine glycosidic angles (*syn, anti*) and, hence, the relative position of the stacked tetrads. In the bimolecular structure, four consecutive thymines are located in each one of the two diagonal loops, interconnected through the backbone, thymines are relatively close each other and one of them is nearly stacked over a guanine of the G-core (Figure 1c). In contrast, thymines in the tetramolecular G4 are located at the two ends of each strand; solution NMR experiments on $(TG_4T)_4/K^+$ did not detect any sign of permanent stacking of thymines in the G-core,[39] meaning that they behave as dangling groups.

The above described geometrical differences in the arrangement of nucleobases in the two G4 structures affects the electronic coupling among them, giving rise to different Franck-Condon states. This is reflected in their absorption spectra, which are compared in Figure 7a. The absorption maximum of OXY/K^+ is red-shifted by 3 nm in respect to its tetra-molecular analog, which, in addition, exhibits a shoulder around 288 nm.

Both the "static" geometrical arrangement and its dynamical behavior should have an important influence on the excited state relaxation, usually requiring small structural modifications.[32] These repercussions concern in particular the excited states involving thymines, due to their different mobility in each system. Thymines have less degrees of freedom in OXY/K^+ because they are located within loops, keeping them relatively close to each other (Figure 1c).[16] As a result, the probability that thymines follow a "monomer-like" decay path is much higher for $(TG_4T)_4/K^+$ compared to OXY/K^+. This is in line with the early time fluorescence anisotropy at 330 nm, corresponding to the emission maximum of this chromophore (Figure 7b).[34] The intensity of the rapidly decaying r(t) signal is higher for the tetramolecular G4

compared to the bimolecular one. However, beyond ~1 ps the two signals coincide. The r_0 value found for $(TG_4T)_4/K^+$ (0.19) falls between the values determined for the stoichiometric mixture of mononucleotides (0.27) and OXY/K^+ (0.14).

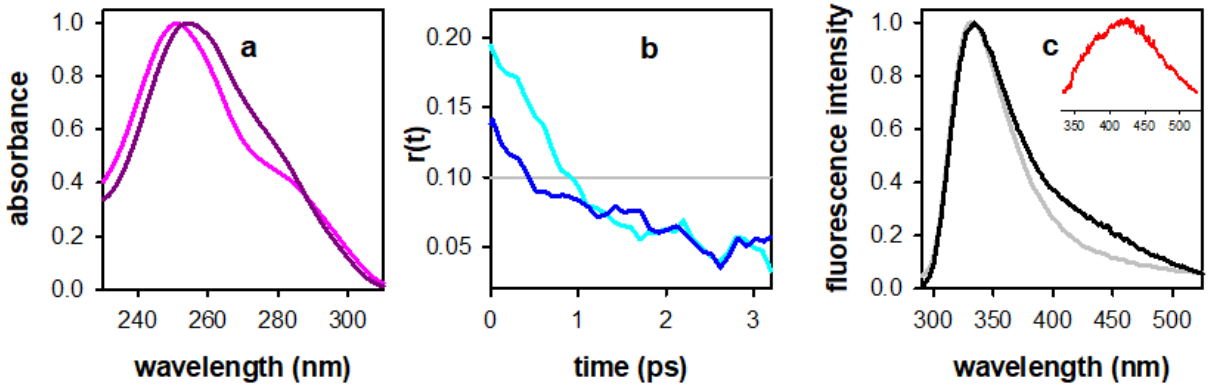

Figure 7. Comparison of selected photophysical properties of OXY/K^+ (dark colors) and $(TG_4T)_4/K^+$ (light colors): (a) steady-state absorption spectra, (b) fluorescence anisotropies at 330 nm and (c) steady-state emission spectra. The spectra in (a) and (c) are normalized in their maxima. The inset in (c) corresponds to the difference between the black and grey spectra.

Figure 7c compares the fluorescence spectra of OXY/K^+ and $(TG_4T)_4/K^+$. Their shapes similar around the maximum but differ at longer wavelengths. Subtraction of the two normalized spectra reveals an emission band peaking at ~445 nm (inset in Figure 7c) and resembling that of excimers and exciplexes.

We first examine if excimer emission may result from guanine-guanine interactions. Previous experimental studies indicate that the topology has not an important influence on the fluorescence of G4 containing K^+ cations in their central cavity. Thus, the fluorescence spectrum of the parallel $(TG_4T)_4/K^+$ structure practically overlaps that of long guanine wires formed by folding of a single guanine strand composed of 2800 guanines (see Figure 2 in reference [23]), for which an all-parallel arrangement is precluded.[40,41]

At a second step, we consider the involvement of thymines in the excimer/exciplex emission. We distinguish two possibilities: (i) between a thymine and a neighboring guanine, shown in

violet in Figure 1c, which are nearly stacked, and (ii) two close lying thymines, encircled in red in Figure 1c. Quantum chemistry calculations showed that excited state relaxation in TEL21/Na^+ may lead to a $G^+ \rightarrow T^-$ CT state.[26] The same type of calculations also showed population of CT excited states in stacked thymine dinucleotides.[42] As mentioned previously, ideal CT states, devoid of oscillator strength, are not detectable by fluorescence. However, deviations from the optimal CT geometry, due to constrains imposed by the backbone and/or direct interaction with the K^+ cations, reported for OXY/K^+,[16] may give rise to weakly emitting states. From the experimental side, a study on monomolecular G4 containing just one thymine per loop, reported a well-defined emission band peaking at 380 nm, assigned to thymine-guanine interactions.[8] As far as thymine-thymine excimers are concerned, their signature should be present in the fluorescence d(T_{20}) single strands.[43,44] Indeed, subtraction of the TMP fluorescence spectrum from that of the single strand results in an emission band peaking at the same position as that of the excimer/exciplex emission of OXY/K^+. Moreover, the fluorescence of d(T_{20}) and OXY/K^+ at 450 nm exhibit the same decay pattern on the ns time-domain (Figure 8b). These similarities strongly indicate emission from of thymine-thymine excimers. However, the two bands in Figure 8a do not thoroughly overlap. The relative shifts observed in the blue and the red sides could be simply due to different conformational constrains in the two systems. These are expected to be less important in the single strand, allowing evolution of the excitation toward lower energies. In addition, the higher intensity of the OXY/K^+ emission at the blue side could be due to a contribution of guanine-thymine exciplexes, appearing at shorter wavelengths.[8]

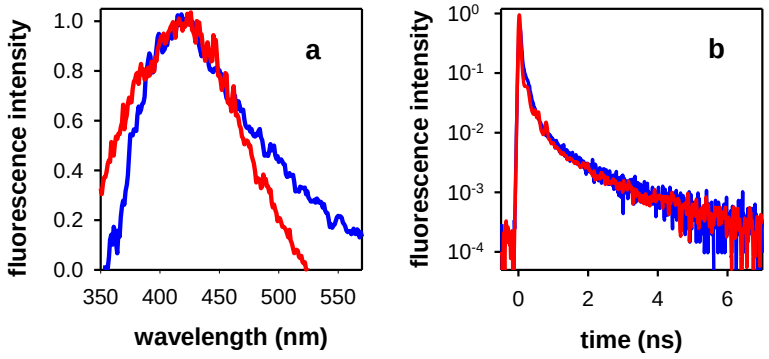

Figure 8: Comparison of the low-energy fluorescence of OXY/K^+ (red) for and d(T_{20}) blue (data from reference [43]). The red spectrum in (a) is that of the inset in Figure 7c, while the blue is the difference between the d(T_{20}) and TMP fluorescence spectra.

The fluorescence quantum yield of OXY/K^+ (5.8×10^{-4}) is 50% higher than that of $(TG_4T)_4/K^+$ (4.0×10^{-4}). The additional "excimer" band alone cannot account for such a difference. This could rather be due to the participation of thymines to exciton states. Moreover, it is possible that the existence of eight 8 ends in $(TG_4T)_4/K^+$, instead of 4 in OXY/K^+, accelerates the localization of exciton states. In this respect, we remark that the ϕ of OXY/K^+ falls between the values reported for monomolecular G4 ($\geq 6.8\times10^{-4}$) and tetramolecular G4 ($\leq 5.1\times10^{-4}$).[6,8] However, a systematic study performed to this end is needed before drawing a positive conclusion concerning this effect.

High energy long-lived emission. The occurrence of a weak amplitude component at the blue part of the spectrum decaying on the ns time-scale (Figures 4a and 4c) is surprising. This type of emission was reported for duplexes,[6,45] being particularly visible for $d(GC)_n\bullet d(GC)_n$, completely dominating its fluorescence spectrum.[46] But this is the first time that a high-energy long-lived emission is detected for a G4. Quantum chemistry calculations for model duplexes with alternating guanine-cytosine[47] and adenine-thymine[48] sequences suggested that such an emission may originate from mixed excitons extended at least over two base-pairs and characterized by a

weak CT between a purine and a pyrimidine; their population has been associated with symmetry effects. At this stage, it is difficult to speculate about the geometrical and electronic features of the excited high energy long-lived emitting states in OXY/K^+. We simply remark that two specific structural features of its structure are absent from the G4 studied previously by the same methodology and do not exhibit such emission. First, we deal with a symmetrical bimolecular G-quadruplex with four tetrads characterized by *syn–anti–syn–anti* glycosidic torsion angles along each strand. Second, we have two diagonal thymine loops. These observations could possibly help to orient future calculations aiming to clarify this point.

Conclusions

The present first fluorescence study on bimolecular G4 revealed, on the one hand, trends similar to those reported for the monomolecular and tetramolecular G4, and on the other, properties specific to this particular structure.

As for the other G4 studied previously[13,22-26] from the femtosecond to the nanosecond time-scales, we found that ultrafast excitation transport takes place among the nucleobases of OXY/K^+, due to internal conversion among the exciton states populated by photon absorption. The major part of the photons, stemming from $\pi\pi^*$ states, with possibly some weak charge transfer character, are emitted before 100 ps.

A specific property detected only for OXY/K^+ is a weak amplitude fluorescent component appearing on the blue side of the spectrum which decays on a ns time-scale, reported so far only for double strands. As this component could be potentially correlated with the symmetrical structure of OXY/K^+ formed by two identical DNA strands, it would be interesting to examine whether it is also present for other G4 characterized by similar symmetry elements.

The interaction between thymines in the loops gives rise to a weak emission peaking around 445 nm, well separated from the fluorescence maximum located at 334 nm. The location of the thymines in loops can also be correlated with the ultrafast excitation transfer: this process is more efficient in OXY/K^+ compared to previously studied G4, which all possess at least one dangling end. Whether this specificity is exclusively related to the presence of two diagonal loops in OXY/K^+, or if the location of peripheral nucleobases in other types of loops, such as lateral or propeller,[9] could produce the same effect, remains to be elucidated.

ASSOCIATED CONTENT

Supporting Information. Experimental details. Fits of the fluorescence decays.

AUTHOR INFORMATION

Corresponding Author

*dimitra.markovitsi@universite-paris-saclay.fr

Present Addresses

†If an author's address is different than the one given in the affiliation line, this information may be included here.

Funding Sources

This work received funding by the European Program H2020 MSCA ITN (grant No. 765266 – LightDyNAmics project).

ACKNOWLEDGMENT

We thank Dr. Lara Martinez-Fernandez for helpful discussions and assistance for drawing the G4 structures.

REFERENCES

(1) Blackburn, E. H.; Epel, E. S.; Lin, J. Human telomere biology: A contributory and interactive factor in aging, disease risks, and protection. *Science* **2015**, *350*, 1193-1198.

(2) Gao, J.; Pickett, H. A. Targeting telomeres: advances in telomere maintenance mechanism-specific cancer therapies. *Nat. Rev. Cancer* **2022**, *22*, 515-532.

(3) Mergny, J. L.; Sen, D. DNA Quadruple Helices in Nanotechnology. *Chem. Rev.* **2019**, *119*, 6290-6325.

(4) Xiang, X.; Li, Y.; Ling, L.; Bao, Y.; Su, Y.; Guo, X. Label-free and dye-free detection of target DNA based on intrinsic fluorescence of the (3+1) interlocked bimolecular G-quadruplexes. *Sens. Actuators B Chem.* **2019**, *290*, 68-72.

(5) Zuffo, M.; Gandolfini, A.; Heddi, B.; Granzhan, A. Harnessing intrinsic fluorescence for typing of secondary structures of DNA. *Nucl. Ac. Res.* **2020**, *48*, e61.

(6) Gustavsson, T.; Markovitsi, D. Fundamentals of the Intrinsic DNA Fluorescence. *Acc. Chem. Res.* **2021**, *54*, 1226-1235.

(7) Improta, R.; Santoro, F.; Blancafort, L. Quantum Mechanical Studies on the Photophysics and the Photochemistry of Nucleic Acids and Nucleobases. *Chem. Rev.* **2016**, *116*, 3540-3593.

(8) Sherlock, M. E.; Rumble, C. A.; Kwok, C. K.; Breffke, J.; Maroncelli, M.; Bevilacqua, P. C. Steady-State and Time-Resolved Studies into the Origin of the Intrinsic Fluorescence of G-Quadruplexes. *J. Phys. Chem. B* **2016**, *120*, 5146-5158.

(9) Basics of G-quadruplex structures. https://ericlarg4.github.io/Distill_section/docs/guideline.html (accessed December, 5 2022).

(10) Kwok, C. K.; Sherlock, M. E.; Bevilacqua, P. C. Effect of Loop Sequence and Loop Length on the Intrinsic Fluorescence of G-Quadruplexes. *Biochemistry* **2013**, *52*, 3019-3021.

(11) Dao, N. T.; Haselsberger, R.; Michel-Beyerle, M. E.; Phan, A. T. Following G-quadruplex formation by its intrinsic fluorescence. *Febs Letters* **2011**, *585*, 3969-3977.

(12) Gao, S.; Cao, Y.; Yan, Y.; Xiang, X.; Guo, X. Correlations between fluorescence emission and base stacks of nucleic acid G-quadruplexes. *RSC Advances* **2016**, *6*, 94531-94538.

(13) Ma, C. S.; Chan, R. C.-T.; Chan, C. T.-L.; Wong, A. K.-W.; Kwok, W.-M. Real-time Monitoring Excitation Dynamics of Human Telomeric Guanine Quadruplexes: Effect of Folding Topology, Metal Cation, and Confinement by Nanocavity Water Pool. *J. Phys. Chem. Lett.* **2019**, *10*, 7577−7585.

(14) Feng, H.; Kwok, C. K. Spectroscopic analysis reveals the effect of hairpin loop formation on G-quadruplex structures. *RSC Chem. Biol.* **2022**, *3*, 431-435.

(15) Lopez, A.; Liu, J. Probing metal-dependent G-quadruplexes using the intrinsic fluorescence of DNA. *Chem. Comm.* **2022**, *58*, 10225-10228.

(16) Schultze, P.; Hud, N. V.; Smith, F. W.; Feigon, J. The effect of sodium, potassium and ammonium ions on the conformation of the dimeric quadruplex formed by the Oxytricha nova telomere repeat oligonucleotide d(G(4)T(4)G(4)). *Nucl. Ac. Res.* **1999**, *27*, 3018-3028.

(17) Kang, C.; Zhang, X.; Ratliff, R.; Moyzis, R.; Rich, A. Crystal structure of four-stranded Oxytricha telomeric DNA. *Nature* **1992**, *356*, 126–131.

(18) Ida, R.; Wu, G. Direct NMR detection of alkali metal ions bound to G-quadruplex DNA. *J. Am. Chem. Soc.* **2008**, *130*, 3590-3602.

(19) Krafft, C.; Benevides, J. M.; Thomes Jr, G. J. Secondary structure polymorphism in Oxytricha nova telomeric DNA. *Nucleic Acids Research* **2002**, *30*, 3981-3991.

(20) Spackova, N.; Berger, I.; Sponer, J. Nanosecond molecular dynamics simulations of parallel and antiparallel guanine quadruplex DNA molecules. *J. Am. Chem. Soc.* **1999**, *121*, 5519-5534.

(21) Fadrná, E.; Spacková, N.; Stefl, R.; Koca, J.; Cheatham, T.; Sponer, J. Molecular dynamics simulations of Guanine quadruplex loops: advances and force field limitations. *Biophys. J.* **2004**, 277-242.

(22) Miannay, F. A.; Banyasz, A.; Gustavsson, T.; Markovitsi, D. Excited states and energy transfer in G-quadruplexes. *J. Phys. Chem. C* **2009**, *113*, 11760-11765.

(23) Hua, Y.; Changenet-Barret, P.; Improta, R.; Vayá, I.; Gustavsson, T.; Kotlyar, A. B.; Zikich, D.; Šket, P.; Plavec, J.; Markovitsi, D. Cation Effect on the Electronic Excited States of Guanine Nanostructures Studied by Time-Resolved Fluorescence Spectroscopy. *J. Phys. Chem. C* **2012**, *116*, 14682–14689.

(24) Hua, Y.; Changenet-Barret, P.; Gustavsson, T.; Markovitsi, D. The effect of size on the optical properties of guanine nanostructures: a femtosecond to nanosecond study. *Phys. Chem. Chem. Phys.* **2013**, *15*, 7396-7402.

(25) Changenet-Barret, P.; Hua, Y.; Gustavsson, T.; Markovitsi, D. Electronic excitations in G-quadruplexes formed by the human telomeric sequence: a time-resolved fluorescence study. *Photochem. Photobiol.* **2015**, *91*, 759–765.

(26) Martinez-Fernandez, L.; Changenet, P.; Banyasz, A.; Gustavsson, T.; Markovitsi, D.; Improta, R. A Comprehensive Study of Guanine Excited State Relaxation and Photoreactivity in G-Quadruplexes. *J. Phys. Chem. Lett.* **2019**, *10*, 6873-6877.

(27) Changenet-Barret, P.; Emanuele, E.; Gustavsson, T.; Improta, R.; Kotlyar, A. B.; Markovitsi, D.; Vaya, I.; Zakrzewska, K.; Zikich, D. Optical properties of guanine nanowires: experimental and theoretical study. *J. Phys. Chem. C* **2010**, *114*, 14339–14346.

(28) Randazzo, A.; Spada, G. P.; Webba da Silva, M. Circular dichroism of quadruplex structures. *Top. Curr. Chem.* **2013**, *330*, 67–86.

(29) Improta, R. Quantum Mechanical Calculations Unveil the Structure and Properties of the Absorbing and Emitting Excited Electronic States of Guanine Quadruplex. *Chem. Eur. J.* **2014**, *20*, 8106-8115.

(30) Loco, D.; Jurinovich, S.; Di Bari, L.; Mennucci, B. A fast but accurate excitonic simulation of the electronic circular dichroism of nucleic acids: how can it be achieved? *Phys. Chem. Chem. Phys.* **2016**, *18*, 866-877.

(31) Avagliano, D.; Tkaczyk, S.; Sanchez-Murcia, P. A.; Gonzalez, L. Enhanced Rigidity Changes Ultraviolet Absorption: Effect of a Merocyanine Binder on G-Quadruplex Photophysics. *J. Phys. Chem. Lett.* **2020**, *11*, 10212-10218.

(32) Martinez-Fernandez, L.; Esposito, L.; Improta, R. Studying the excited electronic states of guanine rich DNA quadruplexes by quantum mechanical methods: main achievements and perspectives. *Photochem. Photobiol. Sci.* **2020**, *19*, 436-444.

(33) Banyasz, A.; Martinez-Fernandez, L.; Ketola, T.; Muñoz-Losa, A.; Esposito, L.; Markovitsi, D.; Improta, R. Excited State Pathways Leading to Formation of Adenine Dimers. *J. Phys. Chem. Lett.* **2016**, *7*, 2020-2023.

(34) Onidas, D.; Markovitsi, D.; Marguet, S.; Sharonov, A.; Gustavsson, T. Fluorescence properties of DNA nucleosides and nucleotides: a refined steady-state and femtosecond investigation. *J. Phys. Chem. B* **2002**, *106*, 11367-11374.

(35) Karunakaran, V.; Kleinermanns, K.; Improta, R.; Kovalenko, S. A. Photoinduced dynamics of guanosine monophosphate in water from broad-band transient absorption spectroscopy and quantum-chemical calculations. *J. Am. Chem. Soc.* **2009**, *131*, 5839-5850.

(36) Borrego-Varillas, R.; Cerullo, G.; Markovitsi, D. Exciton Trapping Dynamics in DNA Multimers. *J. Phys. Chem. Lett.* **2019**, *10*, 1639−1643.

(37) Albrecht, A. C. Polarizations and assignments of transitions - method of photoselection. *J. Mol. Spectrosc.* **1961**, *6*, 84-108.

(38) Phillips, K.; Dauter, Z.; Murchie, A. I. H.; Lilley, D. M. J.; Luisi, B. The crystal structure of a parallel-stranded guanine tetraplex at 0.95 angstrom resolution. *J. Mol. Biol.* **1997**, *273*, 171-182.

(39) Aboul-ela, F.; Murchie, A. I. H.; Norman, D. G.; Lilley, D. M. J. Solution structure of a parallel-stranded tetraplex formed by d(TG4T) in the presence of sodium ions by nuclear magnetic resonance spectroscopy. *J. Mol. Biol.* **1994**, *243*, 458-471.

(40) Kotlyar, A. B.; Borovok, N.; Molotsky, T.; Cohen, H.; Shapir, E.; Porath, D. Long, monomolecular guanine-based nanowires. *Adv. Mater.* **2005**, *17*, 1901-1905.

(41) Borovok, N.; Iram, N.; Zikich, D.; Ghabboun, J.; Livshits, G. I.; Porath, D.; Kotlyar, A. B. Assembling of G-strands into novel tetra-molecular parallel G4-DNA nanostructures using avidinbiotin recognition. *Nucleic Acids Res.* **2008**, *36*, 5050-5060.

(42) Improta, R. Photophysics and Photochemistry of Thymine Deoxy-Dinucleotide in Water: A PCM/TD-DFT Quantum Mechanical Study. *J. Phys. Chem. B* **2012**, *116*, 14261-14274.

(43) Banyasz, A.; Douki, T.; Improta, R.; Gustavsson, T.; Onidas, D.; Vayá, I.; Perron, M.; Markovitsi, D. Electronic Excited States Responsible for Dimer Formation upon UV

Absorption Directly by Thymine Strands: Joint Experimental and Theoretical Study. *J. Am. Chem. Soc.* **2012**, *134*, 14834–14845.

(44) Kwok, W. M.; Ma, C.; Phillips, D. L. A doorway state leads to photostability or triplet photodamage in thymine DNA. *J. Am. Chem. Soc.* **2008**, *130*, 5131-5139.

(45) Chan, R. C.-T.; Ma, C.; Wong, A. K.-W.; Chan, C. T.-L.; Chow, J. C.-L.; Kwok, W.-M. Dual Time-Scale Proton Transfer and High-Energy, Long-Lived Excitons Unveiled by Broadband Ultrafast Time-Resolved Fluorescence in Adenine-Uracil RNA Duplexes. *J. Phys. Chem. Lett.* **2022**, *13*, 302–311.

(46) Vayá, I.; Miannay, F. A.; Gustavsson, T.; Markovitsi, D. High energy long-lived excited states in DNA double strands. *ChemPhysChem* **2010**, *11*, 987-989.

(47) Huix-Rotllant, M.; Brazard, J.; Improta, R.; Burghardt, I.; Markovitsi, D. Stabilization of mixed Frenkel-charge transfer excitons extended across both strands of guanine-cytosine DNA duplexes *J. Phys. Chem. Lett.* **2015**, *6*, 2247-2251.

(48) Vayá, I.; Brazard, J.; Huix-Rotllant, M.; Thazhathveetil, A.; Lewis, F.; Gustavsson, T.; Burghardt, I.; Improta, R.; Markovitsi, D. High energy long-lived mixed Frenkel – charge transfer excitons: from double-stranded $(AT)_n$ to natural DNA. *Chem. Eur. J.* **2016**, *22*, 4904-4914.